

Novel Four-Point-Probe Design and Nanorobotic Dual Endeffector Strategy for Electrical Characterization of As-grown SWCNT Bundles

V. Eichhorn, S. Fatikow, *Member, IEEE*, O. Sardan Sukas, T. M. Hansen, P. Bøggild, and L. G. Occhipinti

Abstract—In this paper, a novel nanorobotic strategy for non-destructive and direct electrical characterization of as-grown bundles of single-walled carbon nanotubes (SWCNTs) is presented. For this purpose, test patterns of SWCNT bundles having different diameters are grown on a silicon substrate by chemical vapor deposition. A new design of microstructured four-point-probes is proposed and fabricated allowing for direct contacting of vertically aligned bundles of SWCNTs. A nanorobotic setup is upgraded into a dual endeffector system to achieve good electrical contact between four-point-probe and SWCNT bundle and to perform electrical measurements. First experimental results of non-destructive electrical characterization are presented and discussed.

I. INTRODUCTION

The ongoing miniaturization of integrated circuits is reaching the limit of traditional copper interconnects in terms of structurability and electrical conductivity. Carbon nanotubes (CNTs) and especially bundles of single-walled carbon nanotubes (SWCNTs) are one of the most promising material to replace and outperform classical copper interconnects [1], [2]. Furthermore, carbon nanotubes have a huge potential in micro- and nanoelectronics [3], [4] and nanosensor applications [5], [6]. But to bring SWCNTs into interconnect applications, a non-destructive electrical characterization method is required enabling direct measurements on as-grown SWCNT bundles. Vice-versa, such a technique can be used to optimize the fabrication process of CNTs and to increase the efficiency of direct growth techniques for horizontal and vertical CNT interconnects.

For the fabrication of CNTs, mainly three different techniques are available. Laser ablation [7] and arc-discharge [8] methods can be used to produce huge amount of CNTs with high yield and only few defects such as Stone-Wales defects. But these two methods only provide clusters of CNTs with undefined orientation and various geometries of individual CNTs. However, chemical vapor deposition (CVD)-based techniques have the advantage of producing CNTs with definable geometries and well defined orientations [9]. In this paper, we describe a CVD-based technique that can be used to grow arrays of SWCNT bundles for testing purposes as well as to directly grow CNT interconnects in the future.

This work is supported by the European Commission: Project NanoHand (IP 034274)

V. Eichhorn and S. Fatikow are with Division Microrobotics and Control Engineering, University of Oldenburg, 26111 Oldenburg, Germany. volkmar.eichhorn@uni-oldenburg.de

O. Sardan Sukas, T. M. Hansen, and P. Bøggild are with DTU Nanotech, Department of Micro and Nanotechnology, Technical University of Denmark. peter.boggild@nanotech.dtu.dk

L. G. Occhipinti is with STMicroelectronics Srl, IMS R&D, Str. Pri-mosole, 50 - 95121 Catania (Italy) luigi.occhipinti@st.com

The most suitable method for reliable characterization of CNTs and prototyping of CNT-based devices is the nanorobotic approach [10], [11], [12]. The development of a nanorobotic system that has been used to perform mechanical characterization of individual multi-walled carbon nanotubes (MWCNTs) has already been presented in [13]. Furthermore, the system facilitates the microgripper-based prototyping of so-called CNT-enhanced AFM supertips [14], [15]. In this paper, we present the further development of this setup into a nanorobotic dual endeffector system able to perform reliable electrical characterization of SWCNT bundles.

In general, electrical characterization of nanotubes and nanowires is challenging since it is hard to mechanically and electrically contact such nanostructures. Furthermore, in case of a two point measurement, the influence of contact resistance between CNT and electrode structure is interfering with the resulting conductivity values. To compensate for the effect of contact resistance, four point measurements can be used [16]. So-called microstructured four-point-probes (4PPs) have already been used to realize electrical measurements on MWCNTs [17], [18]. The traditional design of these 4PPs does not allow for direct contacting of as-grown vertically aligned MWCNTs and SWCNT bundles as it requires a prior process of manipulation of the nanotubes which is in most of the cases time consuming and affecting the structure of the CNTs. To overcome this problem and to realize a non-destructive and direct electrical characterization of SWCNT bundles, novel 4PPs have been designed and fabricated.

In section II, the manufacturing of test patterns of vertically aligned SWCNT bundles is described. In section III, the design and fabrication of the novel 4PPs is presented. The upgrade of the nanorobotic setup into a dual endeffector system is shown in section IV. Experimental results of electrical measurements on SWCNT bundles are discussed in section V. A conclusion and an outlook on upcoming work are given in section VI.

II. MANUFACTURING OF SWCNT BUNDLES

High quality CNTs and reliable CNT growth techniques are a precondition for the fabrication of CNT-based nanoelectronic devices. Among the different growth methods, CVD-based processes are the most commonly used, especially when local growth from patterned catalysts is targeted. In general, the controlled growth of individual CNTs or CNT bundles (both SWCNTs and MWCNTs) is obtained at high temperatures, between 750 °C and 1000 °C, by thermal CVD, or so-called site-selective catalytic chemical vapor deposition

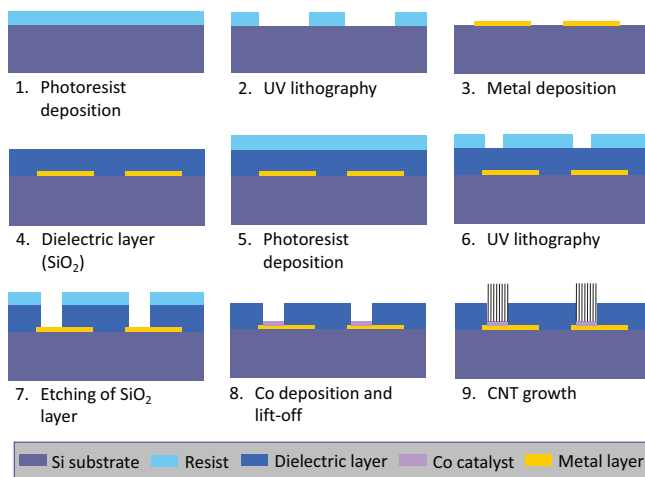


Fig. 1. Manufacturing flow-chart of cleanroom processes for the fabrication of SWCNT bundles containing substrates.

(CCVD) on silicon-based substrates as reported in [19]. High growth temperatures tend to generate side effects such as circular defects that make it challenging to be introduced as a process step in conventional silicon-based manufacturing lines for a broad range of potential applications in microelectronics industry such as advanced interconnects, transistors, integrated circuits, integrated passive components, and field emitter devices. In order to overcome these limitations, CNT films or CNT bundles need to be grown at temperatures below 750°C , in order to keep the compatibility with state-of-the-art IC fabrication technology. This is done by plasma enhanced chemical vapor deposition (PECVD) or by microwave-assisted PECVD, offering a way to obtain high quality CNTs at relatively low temperatures. Among the most critical aspects, it is worth to underline the selection and preparation of catalyst nanoparticles, as well as the appropriate tuning of the gas flow process parameters.

In our experiments, we used e-beam evaporator and sputter to deposit the catalyst. Both sputtering and e-beam evaporation are used for the deposition of catalyst in form of thin films ($\approx 1\text{ nm}$). The use of sputtering or e-beam evaporation, followed by high temperature annealing, also allows for designing and depositing more dedicated catalyst systems, including e.g. bilayer and trilayer catalyst as well as alloy catalyst systems. Indeed, the catalyst system is of vital importance to control CNT growth and quality. More active catalyst will facilitate CNT growth and help to lower the growth temperature. The control of catalyst nanoparticles and their activation will directly impact the diameter of CNTs, their density and chirality distribution. Following catalyst deposition and activation, bundles of SWCNTs are grown by chemical vapor deposition. This process generally consists of four steps: the ramp-up, the annealing, synthesis, and ramp-down process each with different process conditions. For example, using methane gas as carrier for CNT synthesis, the following process parameters are setup to grow SWCNT bundles:

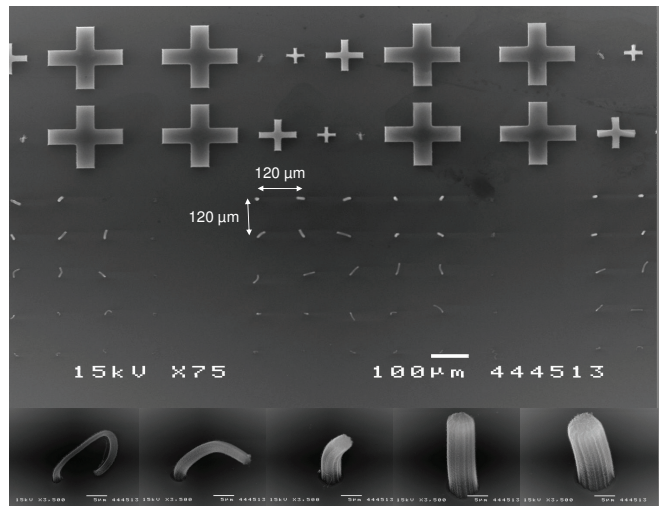


Fig. 2. SEM images of SWCNT bundles grown in via holes of different diameters (from $2\mu\text{m}$ to $10\mu\text{m}$) at well defined positions with a pitch of $120\mu\text{m}$.

- Ramp-up (up to 900°C , 200 sccm H_2 , 60 min)
- Annealing (16 sccm H_2 , 20 min at 900°C)
- Synthesis (140 sccm CH_4 , 10 min at 900°C)
- Ramp-down (200 sccm H_2 until RT, $P=750\text{ torr}$).

In order to develop CNT containing substrates and test structures for the characterization experiments reported in this paper, a dedicated process flow-chart has been developed, which is conceived to obtain regular arrays of SWCNT bundles grown in via holes of different diameters. Fig. 1 shows the schematic flow-chart used for the development of vertically aligned SWCNT bundles in via holes, for testing purposes. The thickness of the dielectric layer for this specific sample is of 500 nm .

As shown in the Fig. 2, the obtained test chip contains arrays of SWCNT bundles with different length that have been grown in via holes of different diameters (from $2\mu\text{m}$ to $10\mu\text{m}$) at well defined positions, with a pitch of $120\mu\text{m}$, in order to ease the nanorobotic approach of 4PPs for electrical characterization. Additional position marks are embedded in the test chip for easily locating SWCNT bundle arrays at low SEM magnifications.

III. DESIGN AND FABRICATION OF NOVEL 4PPS

Conventional 4PPs are designed to perform high-resolution wafer probing and sheet resistance measurements [20] by approaching and contacting the 4PP onto a wafer surface. However, these 4PPs cannot be used to characterize vertically aligned nanotubes or nanowires that are grown on a substrate since the geometrical design prohibits touching. To allow for direct and non-destructive electrical characterization of vertically aligned SWCNT bundles, a novel 4PP design has been developed. Fig. 3a shows the new 4PP concept with L-shaped endeffector tips and the intended approach to an as-grown nanotube or nanowire.

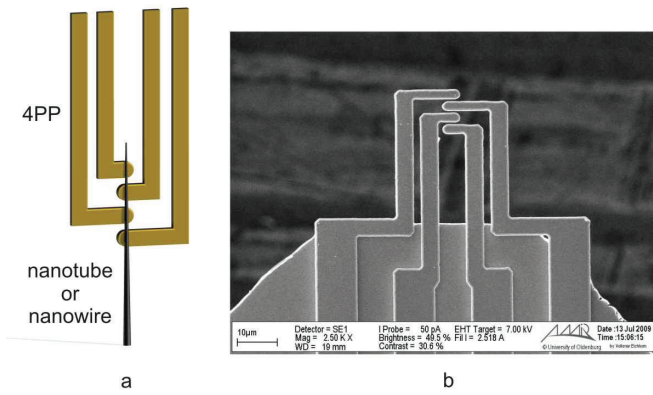


Fig. 3. Novel 4PP design for direct characterization of as-grown SWCNT bundles. Strategy of direct contacting of as grown nanotubes or nanowires (a). SEM image showing the resulting 4PP having an electrode pitch of $3\ \mu\text{m}$ (b).

The 4PPs have been fabricated using standard silicon microfabrication (compare Fig. 4). A $340\ \mu\text{m}$ thick Si(100) 4 inch wafer with $1\ \mu\text{m}$ device layer of SiO_2 is spin coated with a $0.6\ \mu\text{m}$ thick layer of photoresist. The 4PP mask layout is transferred to the resist layer through a negative UV lithography process. Following deposition and lift off of a $75\ \text{nm}$ thick chromium layer as an etch mask, the electrode structures are defined by reactive ion etching (RIE) of the SiO_2 device layer throughout its thickness. After the chromium mask is removed in oxygen plasma, a $350\ \text{nm}$ thick layer of low stress silicon nitride is deposited on both sides of the wafer by low pressure chemical vapor deposition (LPCVD). The backside of the silicon wafer is spin coated with a $1.5\ \mu\text{m}$ thick photoresist layer. The backside mask layout, which defines individual carrier chips, is transferred to the resist layer through a positive UV lithography process, and then to the silicon nitride layer by RIE. The carrier chips are released by KOH etching and the nitride layer on the front side of the wafer is removed by RIE.

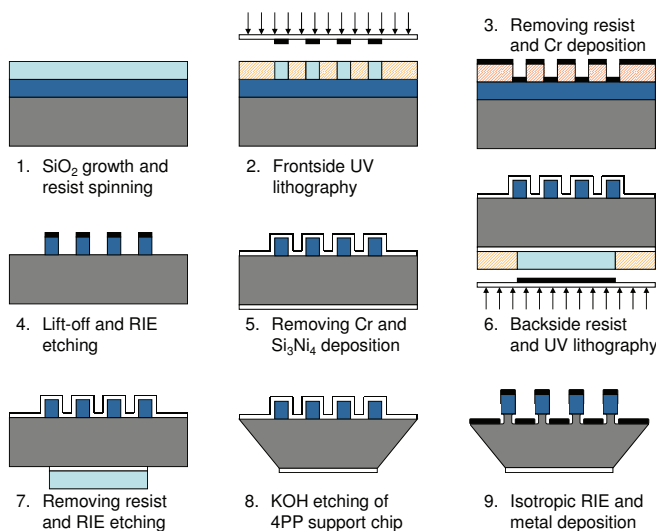


Fig. 4. Manufacturing flow-chart of cleanroom processes for the fabrication of the novel 4PP design.

Finally, $25\ \text{nm}$ titanium and $100\ \text{nm}$ gold is deposited on the front side of the wafer by e-beam deposition as a conductive layer. Fig. 3b shows the SEM image of a resulting 4PP having an electrode pitch of $3\ \mu\text{m}$. 4PPs with different pitches have been fabricated ranging from $1.5\ \mu\text{m}$ to $4\ \mu\text{m}$ thus requiring a minimum length of the analyzed nanotube or nanowire of about $4.5\ \mu\text{m}$.

To connect and mount the 4PPs to the nanorobotic system, the 4PP support chip is glued onto a ceramic substrate with printed gold pads. The 4PP contacts of the support chip are wire-bonded to the gold pads. The ceramic substrate fits into a standard zero insertion force socket which is mounted to the nanorobotic actuator (compare section IV). This plug-and-play system enables easy and quick exchange of different 4PPs.

IV. DUAL ENDEFFECTOR SYSTEM AND STRATEGY FOR ELECTRICAL CHARACTERIZATION

First experiments have been performed with the nanorobotic system described in [15]. For this purpose, the 4PP has been mounted to the micropositioning stage and approached to the as-grown SWCNT bundles that were fixed to the nanopositioning stage. However, no electrical contact could be achieved by only pushing the 4PP against the SWCNT bundle.

For this reason, a dual endeffector system and strategy has been developed allowing for electrical characterization of as-grown SWCNTs bundles by using an etched tungsten tip (STM tip) as second endeffector for assuring good mechanical and electrical contact between CNT bundle and 4PP. Fig. 5 shows the new dual endeffector system being integrated onto the motorized stage of a LEO 1450 SEM.

The setup uses a PI (Physik Instrumente) three-axis nanopositioning stage serving as sample holder for the CNT

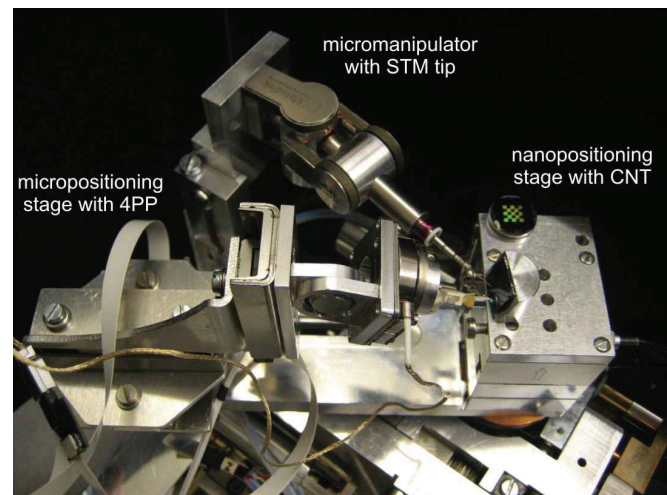


Fig. 5. Dual endeffector system for electrical characterization of as-grown SWCNT bundles. The nanorobotic system consists of three actuator units: A micropositioning stage and a micromanipulator both for positioning the endeffectors (4PP and STM tip) and a nanopositioning stage for moving the sample (SWCNT bundles).

bundles and offering closed-loop actuation with a smallest step size of 1.5 nm and a range of 50 μm . The 4PP is mounted to a SmarAct micropositioning stage consisting of three linear axes with integrated sensors and a rotational axis. This stage offers an overall stroke of 30 mm with minimal step size between 50 and 500 nm. Another Kleindiek micromanipulator with two rotational and a linear degree of freedom is used to position the assisting STM tip. The micromanipulator has a resolution of 5 nm for the rotational axes and 0.25 nm for the linear axis, with an overall working space of 100 cm^3 .

The nanorobotic strategy for electrical characterization of SWCNT bundles is depicted in Fig. 6. The first step is to center the whole setup with respect to the electron beam by using the SEM stage. Then, the sample and both endeffectors are brought into the SEM's region of interest (compare Fig. 6a) by performing several zoom-and-center steps. Afterwards, the micropositioning and nanopositioning stage are used to coarse and fine approach the 4PP to the as-grown SWCNT bundle (see Fig. 6b). Finally, the micromanipulator is used to bring the STM tip close to the SWCNT bundle (compare Fig. 6c) and to create electrical contact by pushing the CNT bundle against the 4PP (see Fig. 6d). The electrical measurements are performed by using an Agilent semiconductor device analyzer B1500A. While the I-V curves are being acquired the electron beam of the SEM is blanked to avoid interaction.

V. EXPERIMENTAL RESULTS

The electrical characterization of nanotubes and nanowires is challenging since it is difficult to mechanically and electrically contact these nanostructures. In addition, the influence of contact resistance between CNT and electrode structure is interfering with the resulting conductivity in case of a two-point measurement. To overcome this problem and to eliminate the influence of contact resistance so-called four point measurements are used [16]. Fig. 7 shows the principle of electrical four-point measurements. The device under test (DUT) is contacted by four individual electrodes having equidistant pitches. An electrical current is driven by the two outer electrodes and the resulting voltage drop is measured by the two inner electrodes. Because this is a currentless measurement of the voltage drop, the contact resistance is not influencing the overall measurement. The idea of four point measurements is also valid for quasi ballistic conductors such as SWCNTs [21].

In general, the *Landauer formula* describes the conductance of ballistic conductors:

$$G = \frac{2e^2}{h} MT, \quad (1)$$

where M is the number of transversal modes within the ballistic conductor and T is the transmission probability. The total resistance can be seen as an interface of the contact resistance G_C^{-1} in series with the resistance of the ballistic conductor G_S^{-1} . Therefore, the conductance of the ballistic conductor itself is given by:

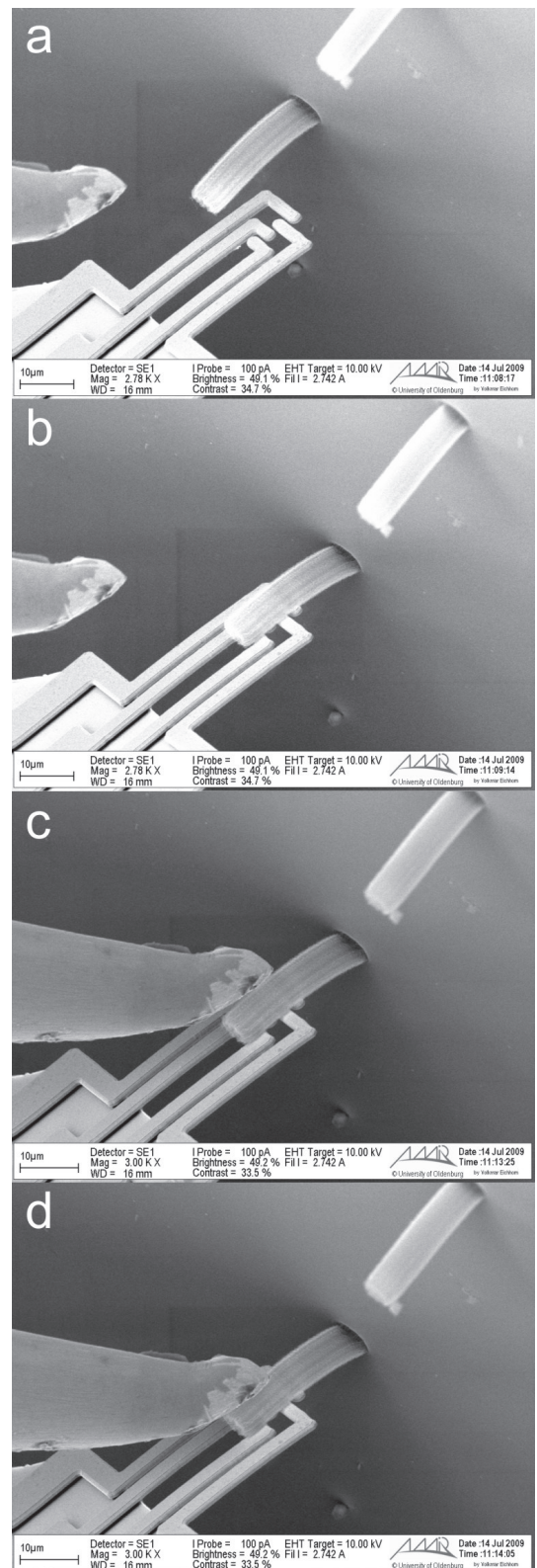


Fig. 6. SEM images showing a typical nanorobotic handling sequence of approaching and contacting 4PP, SWCNT bundle and STM tip. Centering of ROI and coarse approach of sample and endeffectors (a). Fine approach of 4PP and SWCNT bundle (b). Fine approach of STM tip (c) and creation of electrical contact by pushing the STM tip against SWCNT bundle and 4PP (d).

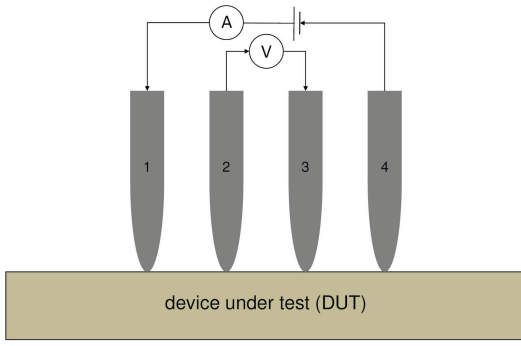


Fig. 7. Principle of electrical four point measurements. An electrical current is driven by the two outer electrodes and the resulting voltage drop is measured by the two inner electrodes.

$$G_S = \frac{2e^2 M}{h} \frac{T}{1-T}. \quad (2)$$

The *Buettiker formula* extends the formalism given above in order to describe the current flow within a ballistic conductor for multiple terminal measurements:

$$I_p = \sum_q^N G_{pq} [V_p - V_q] \quad \text{with} \quad G_{pq} = \frac{2e^2}{h} \bar{T}_{p \leftrightarrow q}. \quad (3)$$

In case of a four point measurement, where the current is driven by the two outer terminals and the voltage drop is measured at the two inner terminals, equation 3 can be rewritten as:

$$\begin{Bmatrix} I_1 \\ I_2 \\ I_3 \end{Bmatrix} = \begin{bmatrix} G_{12}+G_{13} & -G_{12} & -G_{13} \\ -G_{21} & G_{21}+G_{23} & -G_{23} \\ -G_{31} & -G_{32} & G_{31}+G_{32} \end{bmatrix} \begin{Bmatrix} V_1 \\ V_2 \\ V_3 \end{Bmatrix} \quad (4)$$

assuming that the voltage at terminal 4 is equal to zero ($V_4 = 0$). Finally, the measured resistance R in Figure 7 is given by:

$$R = \frac{V}{I} = \left[\frac{V_2 - V_3}{I_1} \right]_{I_2=I_3=0}. \quad (5)$$

The novel 4PP design presented in Section III has been used to perform non-destructive electrical characterization of as-grown SWCNTs bundles. According to Fig. 6, SWCNT bundles have been directly contacted and I-V curves have been recorded. The semiconductor device analyzer has been used to drive an electrical current from $-250 \mu\text{A}$ to $+250 \mu\text{A}$ through the two outer electrodes while measuring the voltage drop at the two inner electrodes. Fig. 8 shows the resulting characteristic I-V curve for a single measurement of a SWCNT bundle with a diameter of $6 \mu\text{m}$. The I-V curves for V_2 and V_3 show a non-ohmic behavior indicating that the given SWCNT bundles consist of a mixture of metallic and semiconducting nanotubes. The calculated resistance according to equation 5 is thus depending on the applied current and ranges from 215Ω to 240Ω for this single measurement.

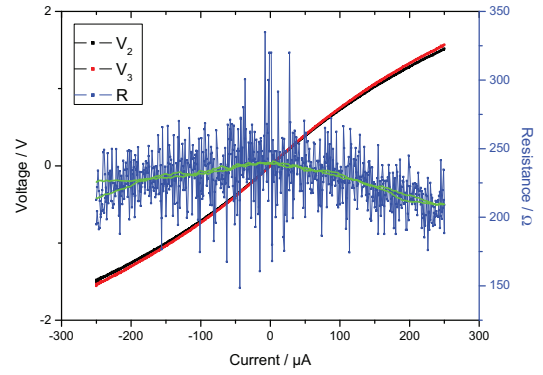


Fig. 8. Resulting I-V curves and calculated resistance for a single electrical characterization of a SWCNT bundle with $6 \mu\text{m}$ diameter.

To verify the reliability of the new L-shaped 4PP strategy, multiple measurements have been performed on one SWCNT bundle. For each measurement the 4PP has been newly approached to the SWCNT bundle and the STM tip has been pushed against the bundle with various forces. Fig. 9 shows the resulting resistance curves. The four measurements show very low variance even for a different contact pressure (compare red and blue curves) and lead to an average resistance between 210Ω and 260Ω .

Calculating the resistivity for the given SWCNT bundles is not reasonable since the resistance for a ballistic conductor should be independent on the length. In reality, the electron mean free path of metallic SWCNTs is about $1 \mu\text{m}$ [22]. For that reason only a quasi ballistic transport can be expected for the given SWCNT bundles. However, for detailed interpretation of the resulting resistance in relation to the SWCNT bundle's geometry it would be necessary to do a detailed analysis of how the current flow is distributed over the bundle since it is connected from the side.

It is important to mention, that the presented strategy provides a possibility for characterizing as-grown SWCNT bundles without destroying the specimen. This technique can pave the way for optimizing the CVD-based fabrication process and allow for prototyping of CNT-based nanoelectronic devices. For future realization of CNT application in horizontal and vertical interconnects, it is important to develop a fabrication technology for producing pure metallic SWCNT bundles hopefully achieving the foreseen performance of ideal SWCNT bundles.

VI. CONCLUSIONS AND FUTURE WORKS

The development and fabrication of a novel four-point-probe design for direct electrical characterization of as-grown bundles of SWCNTs has been presented. A CVD-based method for fabricating arrays of vertically aligned SWCNT bundles has been described. Using this technique, special test patterns of SWCNT bundles with different diameters have been grown. The novel 4PPs and SWCNT samples have been integrated into an upgraded nanorobotic system. The system has been used to develop a dual endeffector strategy allowing for non-destructive electrical characteri-

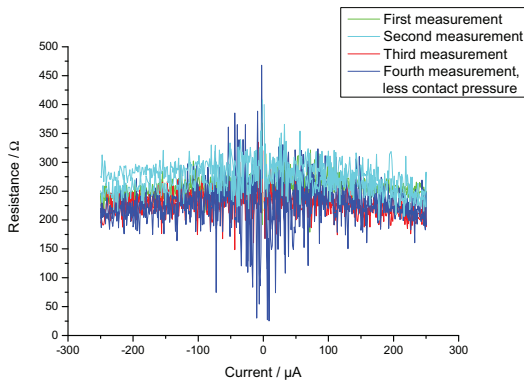


Fig. 9. Multiple electrical measurements of one SWCNT bundle. For each measurement the 4PP has been newly approached to the SWCNT bundle.

zation of SWCNT bundles. A proof-of-principle has been done by measuring characteristic I-V curves and calculating the resulting resistance of SWCNT bundles. The presented nanorobotic strategy and 4PP tool offer a technique for non-destructive and reliable electrical characterization of as-grown nanotubes. Vice-versa, the described technology will allow for prototyping of CNT-based nanoelectronic devices as well as for optimization of direct growth processes for CNT interconnects.

Detailed electrical measurements on SWCNT bundles with different diameters will be performed to analyze the resistance's dependence on the bundle's diameter. For this purpose, the presented nanorobotic system will be embedded into a special control architecture enabling automation of the electrical characterization sequence [23]. In addition, special object recognition and tracking algorithms [24] will be applied to realize SEM-based visual feedback for closed-loop control of all actuators. Furthermore, depth detection techniques presented in [25] have to be adapted enabling the automation of the z-approach between sample and end-effectors. This will lead to a nanorobotic system for rapid characterization of as-grown CNTs and give the opportunity to optimize and increase the efficiency of today's fabrication technologies.

VII. ACKNOWLEDGMENTS

The authors gratefully acknowledge the fruitful discussions within the NanoHand consortium and the support by the DTU Danchip cleanroom team.

REFERENCES

- [1] N. Srivastava, H. Li, F. Kreupl, and K. Banerjee, "On the Applicability of Single-Walled Carbon Nanotubes as VLSI Interconnects," *IEEE Transactions on Nanotechnology*, vol. 8, no. 4, pp. 542–559, 2009.
- [2] C. Rutherglen and P. Burke, "Nanoelectromagnetics: Circuit and Electromagnetic Properties of Carbon Nanotubes," *Small*, vol. 5, no. 8, pp. 884–906, 2009.
- [3] P. Avouris, J. Appenzeller, R. Martel, and S. J. Wind, "Carbon nanotube electronics," *Proceedings of the IEEE*, vol. 91, no. 11, pp. 1772–1784, November 2003.
- [4] W. Hoenlein, F. Kreupl, G. S. Duesberg, A. P. Graham, M. Liebau, R. V. Seidel, and E. Unger, "Carbon Nanotube Applications in Microelectronics," *IEEE Transactions on Components and Packaging Technologies*, vol. 27, no. 4, pp. 629–634, December 2004.

- [5] B. Mahar, C. Laslau, R. Yip, and Y. Sun, "Development of Carbon Nanotube-Based Sensors - A Review," *IEEE Sensors Journal*, vol. 7, no. 2, pp. 266–284, 2007.
- [6] N. Sinha, J. Ma, and J. T. W. Yeow, "Carbon Nanotube-Based Sensors," *Journal of Nanoscience and Nanotechnology*, vol. 6, p. 573590, 2006. [Online]. Available: <http://biomems.uwaterloo.ca/papers/JNN.pdf>
- [7] T. Guo, P. Nikolaev, A. Thess, D. T. Colbert, and R. E. Smalley, "Catalytic growth of single-walled nanotubes by laser vaporization," *Chemical Physics Letters*, vol. 243, pp. 49–54, 1995.
- [8] T. W. Ebbesen and P. M. Ajayan, "Large-scale synthesis of carbon nanotubes," *Nature*, vol. 358, pp. 220–222, 1992.
- [9] K. B. K. Teo, M. Chhowalla, G. A. J. Amaratunga, W. I. Milne, D. G. Hasko, G. Pirio, P. Legagneux, F. Wycisk, and D. Pribat, "Uniform patterned growth of carbon nanotubes without surface carbon," *Applied Physics Letters*, vol. 79, no. 10, pp. 1534–1536, 2001.
- [10] T. Fukuda, F. Arai, and L. Dong, "Assembly of Nanodevices With Carbon Nanotubes Through Nanorobotic Manipulations," *Proceedings of the IEEE*, vol. 91, no. 11, pp. 1803–1818, 2003.
- [11] L. Dong and B. J. Nelson, "Robotics in the Small, Part II: Nanorobotics," *IEEE Robotics & Automation Magazine*, vol. 14, no. 3, pp. 111–121, 2007.
- [12] S. Fatikow and V. Eichhorn, "Nanohandling automation: trends and current developments," *Proceedings of the Institution of Mechanical Engineers, Part C: Journal of Mechanical Engineering Science*, vol. 222, no. 7, pp. 1353–1369, 2008.
- [13] V. Eichhorn, K. Carlson, K. N. Andersen, S. Fatikow, and P. Bøggild, "Nanorobotic Manipulation Setup for Pick-and-Place Handling and Nondestructive Characterization of Carbon Nanotubes," in *Proceedings of the 2007 IEEE/RSJ International Conference on Intelligent Robots and Systems, San Diego, CA, USA, 2007*, p. TuA10.4.
- [14] K. Carlson, K. N. Andersen, V. Eichhorn, D. H. Petersen, K. Mølhave, I. Y. Y. Bu, K. B. K. Teo, W. I. Milne, S. Fatikow, and P. Bøggild, "A carbon nanofibre scanning probe assembled using electrothermal microgripper," *Nanotechnology*, vol. 18, no. 34, p. 345501, 2007.
- [15] O. Sardan, V. Eichhorn, D. H. Petersen, S. Fatikow, O. Sigmund, and P. Bøggild, "Rapid prototyping of nanotube-based devices using topology-optimized microgrippers," *Nanotechnology*, vol. 19, p. 495503, 2008.
- [16] F. M. Smits, "Measurement of sheet resistivities with the four point probe," *The Bell System Technical Journal*, vol. 37, pp. 711–718, 1958.
- [17] C. L. Petersen, T. M. Hansen, P. Bøggild, A. Boisen, O. Hansen, T. Hassenkam, and F. Grey, "Scanning microscopic four-point conductivity probes," *Sensors and Actuators A*, vol. 96, pp. 53–58, 2002.
- [18] S. Dohn, K. Mølhave, and P. Bøggild, "Direct Measurement of Resistance of Multiwalled Carbon Nanotubes Using Micro Four-Point Probes," *Sensor Letters*, vol. 3, no. 4, pp. 300–303, 2005.
- [19] R. Angelucci, R. Rizzoli, V. Vinciguerra, M. Fortuna Bevilacqua, S. Guerri, F. Corticelli, and M. Passini, "Growth of carbon nanotubes by Fe-catalyzed chemical vapor processes on silicon-based substrates," *Physica E*, vol. 37, no. 1–2, pp. 11–15, 2006.
- [20] C. L. Petersen, F. Grey, I. Shiraki, and S. Hasegawa, "Microfour-point probe for studying electronic transport through surface states," *Applied Physics Letters*, vol. 77, no. 23, pp. 3782–3784, 2000.
- [21] S. Datta, *Electronic Transport in Mesoscopic Systems*. Cambridge University Press, 1995.
- [22] M. S. Purewal, B. Hee Hong, A. Ravi, B. Chandra, J. Hone, and P. Kim, "Scaling of Resistance and Electron Mean Free Path of Single-Walled Carbon Nanotubes," *Physical Review Letters*, vol. 98, no. 18, p. 186808, 2007.
- [23] D. Jasper, C. Edeler, C. Diederichs, M. Naroska, C. Stolle, and S. Fatikow, "Towards automated robotic nanomanipulation systems," in *Proceedings of IEEE/ASME International Conference on Advanced Intelligent Mechatronics (AIM)*, 2009.
- [24] T. Wortmann, C. Dahmen, R. Tunnell, and S. Fatikow, "Image processing architecture for real-time micro- and nanohandling applications," in *Proceedings of IAPR Conference on Machine Vision Applications (MVA)*, 2009.
- [25] V. Eichhorn, S. Fatikow, T. Wich, C. Dahmen, T. Sievers, K. N. Andersen, K. Carlson, and P. Bøggild, "Depth-detection methods for microgripper based CNT manipulation in a scanning electron microscope," *Journal of Micro-Nano Mechatronics*, vol. 4, pp. 27–36, 2008.